# Generation of a focused hollow beam by an $2\pi$-phase plate and its application in atom or molecule optics

**Yong Xia and Jianping Yin***

*Key Laboratory for Optical and Magnetic Resonance Spectroscopy, Department of Physics, East China Normal University, Shanghai 200062, China*

Received May 24, 2004; revised manuscript received September 30, 2004; accepted October 4, 2004

We propose a new scheme to generate a focusing hollow beam (FHB) by use of an azimuthally distributed $2\pi$-phase plate and a convergent thin lens. From the Fresnel diffraction theory, we calculate the intensity distributions of the FHB in free propagation space and study the relationship between the waist $w_0$ of the incident Gaussian beam (or the focal length $f$ of the lens) and the dark spot size (or the beam radius) at the focal point and the relationship between the maximum radial intensity of the FHB and the dark spot size (or the beam radius) at the focal point, respectively. Our study shows that the FHB can be used to cool and trap neutral atoms by intensity-gradient-induced Sisyphus cooling due to an extremely high intensity gradient of the FHB itself near the focal point, or to guide and focus a cold molecular beam. We also calculate the optical potential of the blue-detuned FHB for $^{85}$Rb atoms and find that in the focal plane, the smaller the dark spot size of the FHB is, the higher the optical potential is, and the greater the corresponding optimal detuning $\delta$ is; these qualities are beneficial to an atomic lens not only because it is profitable to obtain an atomic lens with a higher resolution, but also because it is helpful to reduce the spontaneous photon-scattering effect of atoms in the FHB. 

*OCIS codes:* 020.7010, 050.1940, 120.5060, 220.2560.

## 1. INTRODUCTION

Since the 1990s, a variety of techniques, such as geometrical optical method,[1] mode conversion,[2] optical holography,[3] computer-generated holography,[4] transverse-mode selection[5] and hollow-fiber method,[6] nonlinear optical method,[7,8] and so on, have been used to generate various dark hollow beams (DHBs) with zero central intensity.[6,9] Since the DHB has some novel and unique physical properties such as a barrel-shaped intensity distribution, a helical wave front, and center phase singularity and may carry spin and orbital angular momentum and exhibit spatial propagation invariance, it has many important and wide applications in modern optics and atomic and molecular optics.

As early as 1987, Balykin Letokhov[10] proposed an atomic lens scheme that used a blue-detuned focusing doughnut hollow beam. Afterward, various aberrations of atomic lens composed of the focused doughnut hollow beam were studied theoretically by Gallatin and Gould[11] and McClelland and Scheinfein.[12] Recently, a diffraction-limited dark laser spot was produced with the diffracted field of the $LP_{11}$ mode of a hollow optical fiber.[13] However, this focused $LP_{11}$-mode output beam may be not easy for forming an ideal and useful atomic lens, because the $LP_{11}$ mode does not have a closed doughnutlike intensity profile in the cross section. Therefore it is interesting and worthwhile to generate a focused hollow beam (FHB) and realize an atomic lens with a resolution of several angstroms.

In general, when a Gaussian laser beam or a doughnut hollow beam is focused by a lens, the focused beam near the focal point of the lens will be become a Gaussian one owing to the diffraction effect of the lens (i.e., the constructive interference effect). However, we found that when a Gaussian beam or a hollow beam passes through a special $2\pi$-phase plate and is focused by a thin lens, a FHB with zero axial intensity will be generated as a result of completely destructive interference at the beam center (or at the light axis). Since this kind of hollow beam has a very small dark-spot size (DSS) in the focal plane, it can be used to focus an atomic (or molecular) beam as an atomic (or molecular) lens and to perform atomic (or molecular) lithography, laser cooling, and trapping of neutral atoms and even to study the adiabatic heating and cooling of atoms (molecules) in the blue-detuned FHB owing to adiabatic compression and expansion of guided atomic (or molecular) beam.

In this paper, we propose a new scheme to generate a FHB by use of an optical system composed of an azimuthally distributed $2\pi$-phase plate and a convergent thin lens and discuss some potential applications of the blue-detuned FHB in atomic optics, particularly in atomic lens. In Section 2 we propose a new scheme to generate a FHB by use of a $2\pi$-phase plate and a lens and derive the intensity distribution of the FHB in free space from the Fresnel diffraction equation. In Section 3 we calculate the radial intensity distributions of the FHB behind the lens at the different propagation distance $z$ and discuss the propagation characteristics of the FHB in free space. In Section 4, we study the relationship between the DSS

 

(or $2R_0$) of the FHB and the propagation distance $z$, and the relationship between the DSS (or $2R_0$) of the FHB at the focal point and the waist $w_0$ of the incident Gaussian beam (or the focal length $f$ of the lens). In Section 5 some potential applications of the blue-detuned FHB in atom (or molecule) optics are briefly discussed. The main results and conclusions are summarized in Section 6.

## 2. NEW SCHEME TO GENERATE A FOCUSING HOLLOW BEAM

Figure 1(a) shows the phase distribution of a $2\pi$-phase plate, and its phase $\varphi$ will be continuously changed with the azithmual angle $\theta$ from 0 to $2\pi$, which can be fabricated by use of a similar method in Ref. 14. Figure 1(b) shows a principle scheme to generate the FHB. When a well-collimated Gaussian laser beam with an intensity distribution

$$E(x_0, y_0, z) = A \exp\{-[(x_0^2 + y_0^2)/w_0^2]\}\exp(-ikz) \tag{1}$$

passes through an azimuthally distributed $2\pi$-phase plate, as shown in Fig. 1(a) and is focused by a thin lens with a focal length $f$, a FHB will be produced behind the lens owing to the completely destructive interference effect at the beam center. This generation mechanism of the FHB can be explained as follows. We can see from Fig. 1(a) that the phase difference between two sides of an arbitrary straight line that passes through the circular center of the phase plate is always equal to $\pi$, and the center of the phase plate (i.e., the center of the incident beam) is a symmetric center of this $\pi$ phase deference and is azimuthally distributed, which will result in a completely destructive interference effect at the center of the incident Gaussian beam. Therefore the axial intensity of the output beam will be reduced to zero, and a focused hollow beam will be generated behind both the lens and the phase plate.

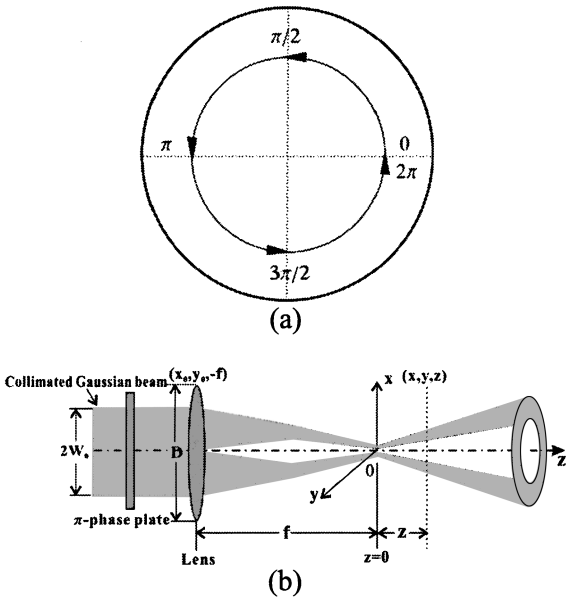


Fig. 1. (a) A $2\pi$-phase plate with a continuous phase changing from 0 to $2\pi$. (b) Principal experimental setup for production of a FHB. $D$ and $f$ are the diameter of the lens and its focal length and $w_0$ is the waist of the collimated Gaussian beam.

From the Fresnel diffraction equation,[15,16] when a collimated Gaussian laser beam passes through both the phase plate and the thin lens, the intensity distribution of the diffraction field behind the lens, in a polar coordinate, can be written as

$$\begin{aligned} E(r, z) = {} & \frac{A \exp\left(\frac{ik}{2z} r^2\right)\exp[ik(z + 2f)]}{i\lambda(z + f)} \\ & \times \int_0^a \int_0^{2\pi} \exp\left(\frac{r_0^2}{w_0^2}\right)\exp\left(\frac{ik}{2f} r_0^2\right) \\ & \times \exp\left[\frac{ik}{2(z + f)} r_0^2\right]\exp\left[-\frac{ik}{(z + f)} r r_0 \cos\theta_0\right] \\ & \times \exp(-i\theta_0) r_0 \mathrm{d}r_0 \mathrm{d}\theta_0, \end{aligned} \tag{2}$$

where $A$ and $w_0$ are the complex amplitude and the waist of the incident collimated Gaussian beam, respectively; $f$ is the focal length of the thin lens; $\lambda$ is the light wavelength; $(x_0, y_0, z)$ and $(x, y, z)$ represent the coordinates on the diffraction aperture plane and the image plane, respectively; $\exp[-ikr_0^2/2f]$ is the phase shift of the thin lens, $z$ is the propagation distance along the beam propagation direction, and $z = 0$ shows the position of the focal plane.

At the focal point of the lens (i.e., when $z = 0$), Eq. (2) can be reduced to

$$\begin{aligned} E(r) = {} & \frac{A \exp\left(\frac{ik}{2z} r^2\right)\exp(2ikf)}{i\lambda f} \\ & \times \int_0^a \int_0^{2\pi} \exp\left(-\frac{r_0^2}{w_0^2}\right)\exp\left(-\frac{ik}{f} r r_0 \cos\theta_0\right) \\ & \times \exp(-i\theta_0) r_0 \mathrm{d}r_0 \mathrm{d}\theta_0, \end{aligned} \tag{3}$$

and then the intensity distribution of the FHB in free space can be given by

$$I(r, z) = |E(r, z)|^2. \tag{4}$$

## 3. PROPAGATION CHARACTERISTICS OF THE FHB IN FREE SPACE

To study the propagation characteristics of the FHB in free space, we must first define two special parameters for the FHB as follows[6,9]:

(1) The DSS, defined as a FWHM of the radial-intensity distribution inside the notch of the FHB.
(2) The beam radius $R_0$, defined as the distance between the position of the maximal radial intensity and the center of the light beam.

From Eqs. (2) and (4), we calculate the intensity distribution of the FHB in free space and study the relationship between the DSS and the propagation distance $z$,

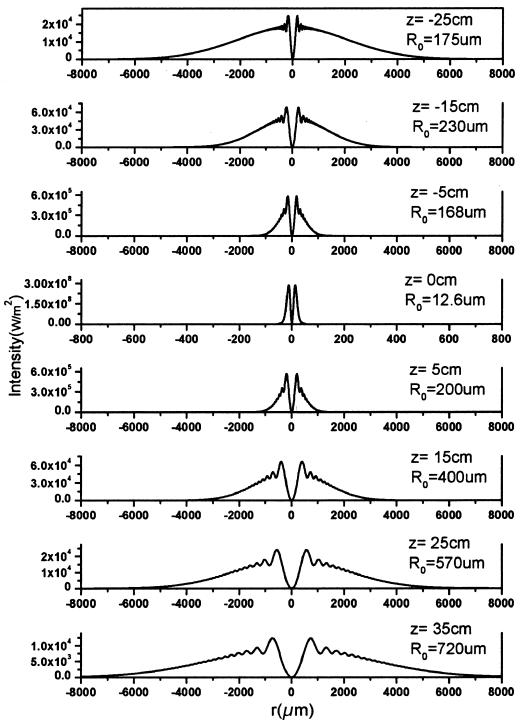


Fig. 2. Radial intensity distributions of the FHB behind the lens at the propagation distance $z = -25, -15, -5, 0, 5, 15, 25,$ and 35 cm. The parameters used in the calculation are $\lambda = 0.78\,\mu$m, $f = 300$ mm, $w_0 = 5$ mm, $P_0 = 1000$ mW, and $D = 50$ mm, respectively.

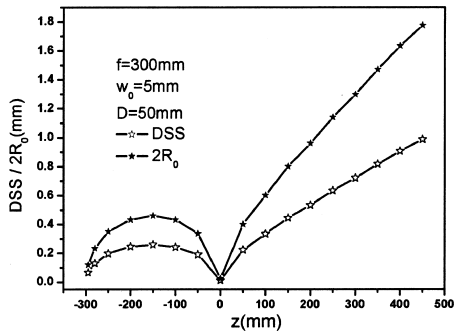


Fig. 3. Relationship between the DSS (or $2R_0$) of the FHB and the propagation distance $z$ for $\lambda = 0.78\,\mu$m and $P_0 = 1000$ mW.

and the results are shown in Figs. 2 and 3, respectively. We can find from Fig. 2 that owing to completely ($r = 0$) and partially ($r \neq 0$) destructive interference effects around the central region of the beam, a FHB with a Gaussian intensity profile will be generated behind the lens; but with the increase of the radial position $r$, the function of the $2\pi$-phase plate for the focused laser beam shows a periodic partially destructive and constructive interference effects, which result in a periodic oscillated modulation on the Gaussian intensity profile except the focal plane of $z = 0$. On the other hand, it can be seen from Figs. 2 and 3 that there is an interesting propagation property of the FHB before the focal plane: With the increase of the propagation distance $z$, the DSS of the FHB first is increased from zero to the maximum value at the position of $z = -f/2$ and then is decreased from the maximum value to the minimum one at the focal point. In particular, the DSS of the FHB at the focal point is extremely small when a larger waist $w$ of the incident Gaussian beam and a shorter focal length $f$ of the lens are chosen, which can be used to focus the guided atomic beam as a novel atomic lens. After the focal plane, the FHB is propagated according to a constant divergent angle, the DSS become larger, and the intensity becomes weaker. In addition, in the exact focal plane, the radial intensity distribution does not have a periodic oscillated modulation, and its intensity profile can be described exactly by the $\mathrm{TEM}_{01}^{*}$ doughnut beam model as follows[17]:

$$I(r) = 4k\,\frac{P_0}{2\pi w_{00}^2}\,\frac{2r^2}{w_{00}^2}\exp\left(-\frac{2r^2}{w_{00}^2}\right), \tag{5}$$

where $P_0$ is the power of the FHB, $w_{00}$ is the beam waist of the FHB in the focal plane of $z = 0$, and $k$ is the fitting parameter, which will be used to correct the change of the peak intensity at $r = R_0$ due to the modulation of the phase plate for the light field; here, $R_0$ is defined as the beam radius.

It is clear from Fig. 2 that the maximum radial intensity of the FHB at the focal point is ~500 times greater than that at the propagation distance $z = \pm 5$ cm. Owing to the extremely high intensity gradient of the FHB near the focal point, the FHB can also be used to cool and trap neutral atoms by intensity-gradient induced Sisyphus cooling.[6]

We compare the radial intensity distributions of the FHB at the propagation distance $z = 15$ cm when the $2\pi$-phase plate is used and when it is not used, and the results are shown in Fig. 4. It can be seen from Fig. 4 that when the $2\pi$-phase plate is not used, the radial intensity distribution of the focused Gaussian beam behind the thin lens is still a Gaussian one; this is due mainly to the diffraction effect of the lens (or the constructive interference effect of the focused laser beam). When the $2\pi$-phase plate is used, the intensity at the light axis is reduced to zero as a result of completely destructive interference at the beam center, whereas the intensity at the other radial position $r$ will be modulated by the periodically, partially destructive, and constructive interfer-

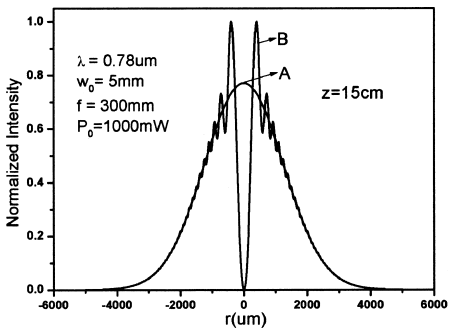


Fig. 4. Radial intensity distribution of the focused Gaussian beam at the propagation distance $z = 15$ cm when a $2\pi$-phase plate is used (curve A) or not used (curve B) for $\lambda = 0.78\,\mu$m, $w_0 = 5$ mm, $f = 300$ mm and $P_0 = 1000$ mW.

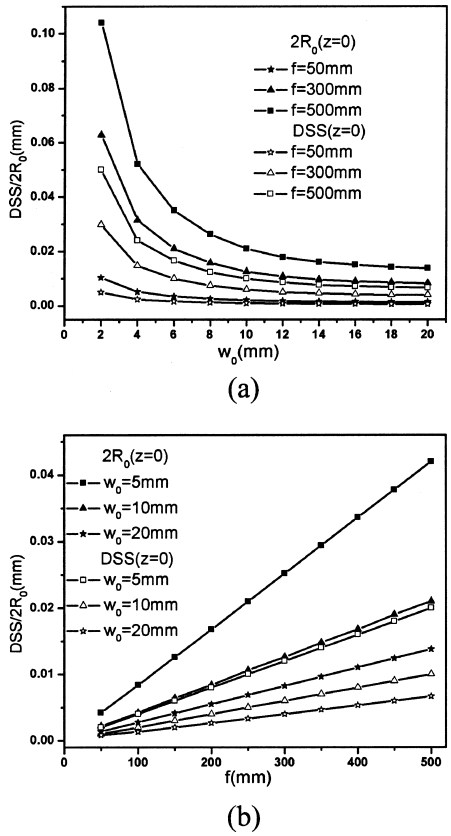


Fig. 5. (a) Relationship between the DSS (or $2R_0$) of the FHB at the focal point $z = 0$ and the waist $w_0$ of the incident Gaussian beam for $f = 50$, 300, and 500 mm. (b) Relationship between the DSS (or $2R_0$) of the FHB at the focal point and the focal length $f$ of the lens for $w_0 = 5$, 10, and 20 mm.

ence effects of the $2\pi$-phase plate for the incident beam. Therefore with an increase of the radial position $r$, the intensity distribution shows a periodically oscillated modulation in the Gaussian intensity profile, which results in a FHB. It can also found from Fig. 4 that the area under the radial intensity distribution curve $A$ of a focused Gaussian beam is equal to one under the radial intensity distribution curve $B$ of the FHB. This shows that the power of the focused Gaussian beam (without the $2\pi$-phase plate) is the same as one of the FHB (with the $2\pi$-phase plate) at the identical propagation distance $z$.

## 4. FOCUSING CHARACTERISTICS OF THE FHB IN THE FOCAL PLANE OF THE LENS

We calculate the intensity distribution of the FHB in the focal plane of $z = 0$ and study the relationship between the DSS (or $2R_0$) of the FHB at the focal point and the waist $w_0$ of the incident collimated Gaussian beam; the results are shown in Fig. 5(a). It is clear from Fig. 5(a) that with an increase of the waist $w_0$ of the incident Gaussian beam, the DSS (or $2R_0$) of the FHB will be reduced rapidly. Just as when the focal length $f = 500$ mm and the waist $w_0$ is increased from $w_0 = 2$ mm to $w_0 = 20$ mm, the DSS will be reduced from 50.0 to 6.6 $\mu$m. When $f = 50$ mm, the DSS will be reduced from 5.0 to 0.66 $\mu$m, which is closed to the diffraction limit $\lambda/2$. We also study the relationship between the DSS (or $2R_0$) of the FHB and the focal length $f$ of the lens, and the results are shown in Fig. 5(b). It is obvious from Fig. 5(b) that when $w_0 = 5$ mm, with the reduction of the focal length $f$ from 500 to 50 mm, the DSS will be linearly decreased from 20.0 to 2.0 $\mu$m. While $w_0 = 20$ mm, the DSS will be decreased from 6.7 to 0.84 $\mu$m with the reduction of the focal length $f$ from 500 to 50 mm.

The maximum radial intensity $I_{\max}$ of the FHB at $r = R_0$ and $z = 0$ is calculated, and the relationship between the $I_{\max}$ of the FHB and the waist $w_0$ of the incident collimated Gaussian beam (and the focal length $f$ of the lens) are studied, and the results are shown in Figs. 6(a) and 6(b), respectively. We can see from Fig. 6 that the larger the waist $w_0$ of the incident Gaussian beam is, the greater the maximum radial intensity of the FHB is; and the shorter the focal length $f$ of the lens is, the greater the maximum radial intensity of the FHB is. Therefore these results show that if the lens with a shorter focal length $f$ and the incident laser beam with a larger waist $w_0$ are chosen, we can obtain a desired FHB with an extremely small DSS, which can be used to form an atomic lens with an extremely high resolution. In addition, since the intensity of the FHB near the focal point of the lens and its intensity gradient are relatively high, the blue-detuned FHB can be used to trap and cool neutral atoms by intensity-gradient induced Sisyphus cool-

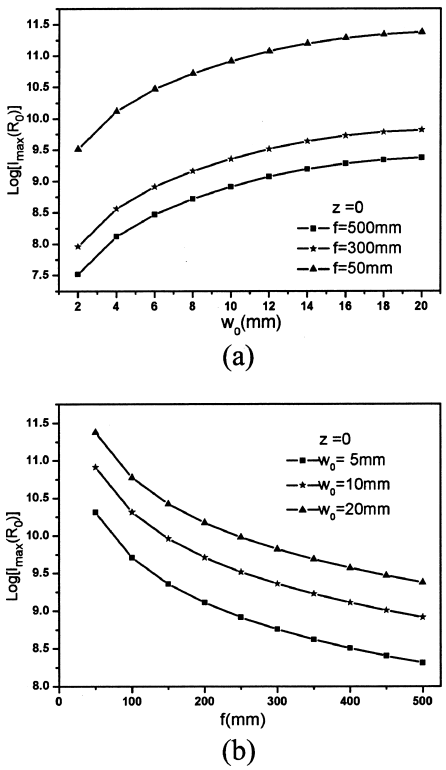


Fig. 6. (a) Relationship between the maximum radial intensity of the FHB at the focal point $z = 0$ and the waist $w_0$ of the incident Gaussian beam for $f = 50$, 300, and 500. (b) Relationship between the maximum radial intensity of the FHB at the focal point $z = 0$ and the focal length $f$ of the lens for $w_0 = 5$, 10, and 20 mm.

ing, even to study the adiabatic heating and cooling of atoms due to adiabatic compression and expansion of guided atomic beam in the FHB.

## 5. POTENTIAL APPLICATIONS OF THE FHB IN ATOMIC OR MOLECULAR OPTICS

### A. Trapping and Cooling of Neutral Atoms

It is well known that when a two-level atom moves in an inhomogeneous light field, it will experience an action from an optical dipole force, resulting in an optical trapping potential[18,19]:

$$U(r) = \frac{\hbar\delta}{2}\ln\left[1 + \frac{I(r)/I_s}{1 + 4(\delta/\Gamma)^2}\right], \tag{6}$$

where $\delta = \omega_l - \omega_a - kv_z$ is the detuning of the laser frequency $\omega_l$ from the atomic resonance frequency $\omega_a$, including the Doppler shift $kv_z$; $I(r)$ is the intensity distribution of the FHB; and $I_s$ and $\Gamma$ are the saturation intensity and the natural linewidth of the atomic transition, respectively. When the light field is blue detuned ($\delta > 0$), the interaction potential is repulsive, and the atoms will be repelled to the minimum of the light field. Therefore atoms will be trapped or guided in a blue-detuned FHB.

Since there is a higher intensity gradient in the standing-wave light or in an evanescent-wave light, atoms moving in the above two light fields will be cooled down to near the recoil temperature by the intensity-gradient induced Sisyphus cooling. Similarly, if there is a higher intensity gradient in the DHB, the DHB can also be used to cool the guided (or trapped) atoms. In 1997, an idea on the DHB-induced Sisyphus cooling (i.e., intensity-gradient cooling) was proposed by Yin *et al.*[6] and was analyzed for a DHB atomic funnel,[20] DHB atomic guiding,[21] a DHB funnel atom trap,[22] a DHB gravito-optical atom trap,[23] and others.[17] We know from the above analysis that the intensity gradient near the focal point of the FHB is quite high, and when a collimated Gaussian beam with a larger waist $w_0$ and a lens with a shorter focal length $f$ are chosen, the intensity gradient of the beam can be further increased. Therefore a more efficient Sisyphus cooling effect for neutral atoms can be obtained near the focal point of the FHB. For example, Fig. 7 shows a novel scheme to trap and cool neutral atoms by use of a pair of crossed blue-detuned FHBs. When cold atoms are loaded from a standard magneto-optical trap (MOT), they will be trapped in a three-dimensional dark hollow region of two crossed FHBs and cooled by FHB intensity-gradient induced Sisyphus cooling.[24]

### B. Focusing of Cold Atomic (Molecular) Beam and its Atomic (Molecular) Lens

From Eq. (6), we calculate the optical potential of the FHB for two-level $^{85}$Rb atoms in the focal plane of $z = 0$, and the results are shown in Figs. 8 and 9. Figure 8 shows the relationship between the optical potential and the detuning $\delta$ of the FHB for the different waist $w_0$ of the incident beam and the focal length $f$ of the lens. It is clear from Fig. 8 that with the reduction of the relative aperture $\beta = w_0/f$ of the optical system, the maximum optical potential will be decreased, and the corresponding optimal detuning $\delta_{\max}$ will be also be reduced rapidly.

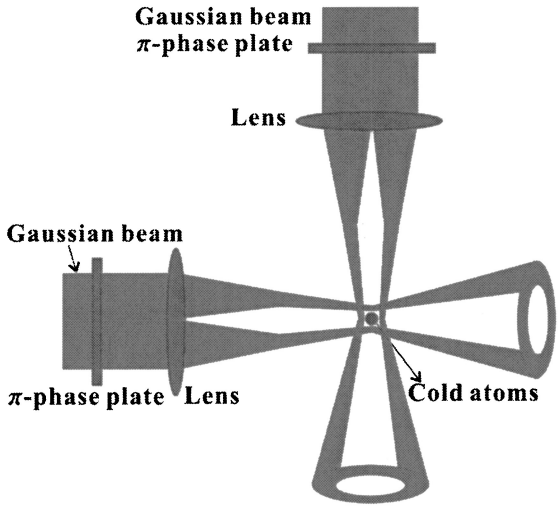


Fig. 7. Principle experimental setup for trapping and cooling neutral atoms by optical potential evaporative cooling.

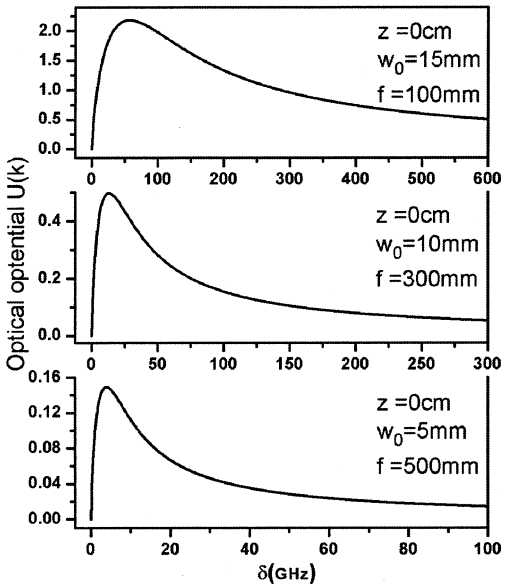


Fig. 8. Relationship between the optical potential of the FHB for $^{85}$Rb atom and its detuning $\delta$ for $\lambda = 0.78\,\mu$m and $P_0 = 1000$ mW, (a) $w_0 = 15$ mm and $f = 100$ mm, (b) $w_0 = 10$ mm and $f = 300$ mm, and (c) $w_0 = 5$ mm and $f = 500$ mm.

Figure 9 shows the radial dependent relationship of the optical potential of the FHB at $z = 0$ for the guided $^{85}$Rb atoms. When $P_0 = 1000$ mW, $w_0 = 15$ mm, $f = 100$ mm, $\delta = 2\pi \times 20$ GHz, $2\pi \times 57$ GHz, and $2\pi \times 100$ GHz; the peak optical potentials (at $r = R_0$) are 1.68, 2.18, and 1.96 K, respectively, which are far higher than the transverse temperature of the cold atomic beam.[25] When cold atoms are guided in the blue-detuned FHB, the guided atomic beam will be focused near the focal point of $z = 0$; in this case, the action of the blue-detuned FHB for the guided cold atoms corresponds to an atomic lens. The aberrations of the atomic lens, including spherical aberration ($\delta_{\text{sph}}$), chromatic aberration

($\delta_{chr}$), spontaneous emission aberration ($\delta_{spont}$), dipole aberrations ($\delta_{dip}$), and diffraction aberration ($\delta_{diffr}$), will affect the smallest spot of the focused atomic beam. That is, the various aberrations will determine the resolution of the atomic lens.[12] So the total aberration of atomic lens will be

$$\delta_{total} = [(\delta_{sph}^2 + \delta_{chr}^2 + \delta_{spont}^2 + \delta_{dip}^2 + \delta_{diffr}^2)]^{1/2}. \quad (7)$$

When the parameters of the incident collimated Gaussian beam are $\lambda = 0.78\,\mu m$, $P_0 = 1000\,mW$, $w_0 = 15\,mm$, $f = 100\,mm$ and $\delta = 2\pi \times 57\,GHz$ respectively, the radius $R_0$ of the FHB is 1.54 $\mu$m at the focal plane, and for the $^{85}Rb\,D_2$ line, if the longitudinal velocity $v_z$ of the guided atomic beam in the FHB is 14 m/s,[25] the focal length $f_{atom}$ of the FHB atomic lens,[12] $f_{atom} = L/\sin(\pi/q)$, is ~9.81 $\mu$m, where $L$ is the Rayleigh length, given by $L = \pi R_0^2/\lambda$; $q$ is the excitation parameters of the atomic lens. In this case, we estimate the various aberrations and its total one from the aberration formulas given in Ref. 12 and Eq. (7) and obtain $\delta_{sph} = 4.455\,nm$, $\delta_{chr} = 0.372\,nm$, $\delta_{spont} = 3.169\,nm$, $\delta_{dip} = 1.236\,nm$, $\delta_{diffr} = 6.652\,nm$, and $\delta_{total} = 8.707\,nm$, respectively. This shows that our FHB can be used to form an atomic lens with a resolution of ~8.71 nm.

In addition, we can see from Fig. 8 that when $P_0 = 1000\,mW$, $w_0 = 5\,mm$ and $f = 500\,mm$ (or $w_0 = 10\,mm$ and $f = 300\,mm$), the maximum optical potential and its optimal detuning are 149 mK and 3.9 GHz (498 mK and 13 GHz), respectively. When $P_0 = 1000\,mW$, $w_0 = 15\,mm$ and $f = 100\,mm$, the maximum optical potential and its optimal detuning are 2.18 K and 57 GHz. This shows that in the focal plane of $z = 0$, the smaller the DSS of the FHB is, the higher the optical potential is, and the greater the corresponding optimal detuning $\delta$ is, which are beneficial to an atomic lens not only because it is profitable for obtaining an atomic lens with a higher resolution, but also because it is helpful for reduction of the spontaneous scattering effects of atoms in the FHB. When a two-level atom moves in a light field, it will experience spontaneous photon scattering, and its scattering rate $S$ is given by[26]:

$$S = \frac{\Gamma|\Omega|^2/2}{2[(\Gamma/2)^2 + \delta^2] + |\Omega|^2}, \quad (8)$$

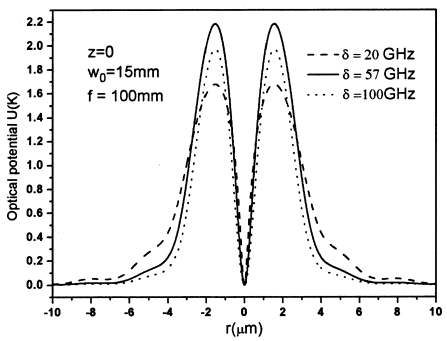


Fig. 9. Optical potential $U(r)$ of the FHB for $^{85}Rb$ atoms versus the radial position $r$ at the propagation distance $z = 0$ cm for $\delta = 20$, 57, and 100 GHz.

here $|\Omega|^2 = I(\mathbf{r})/2I_s\Gamma^2$, where $|\Omega|$ is the Rabi frequency. When $\delta \gg \Omega \gg \Gamma$, the photon scattering rate $S$ can be reduced to

$$S \approx \left(\frac{\Gamma}{2\delta}\right)^2 \frac{I(\mathbf{r})}{2I_s}\Gamma. \quad (9)$$

From Eq. (9), we calculate the photon scattering rate $S$ of the guided atoms in the FHB. When the longitudinal and transverse velocities of cold atomic beam are $v_z = 14\,m/s$ and $v_t = 0.504\,m/s$,[25] and the parameters of the FHB are $P_0 = 1000\,mW$, $\delta = 2\pi \times 57\,GHz$, and $w_0/f = 0.15$, we obtain $S \approx 10.2/s$. Note that the cold atomic beam is guided in the dark region of the blue-detuned FHB and the transverse motion of the guided atoms is confined in a small radius $\bar{r}_{Apd}$ (i.e., average penetrating depth) inside the dark FHB, the averaged intensity $\bar{I}(\bar{r}_{apd})$ occupied by the guided cold atoms is far smaller than one of cold atoms in the red-detuned Gaussian beam with the same parameters, so the photon scattering rate $S$ of atoms in the FHB is lower. If the guiding distance of atoms in the FHB is $L = 50\,cm$, the guiding time will be $t = L/v_z \approx 0.036\,s$, and the corresponding spontaneous photon scattering will be ~0.36 times, which is smaller than 1 time. So the spontaneous photon-scattering effect of atoms in our FHB can be nearly neglected.

It is clear from the above analysis that when an optical system with a larger relative aperture $\beta(=w_0/f)$ is chosen, we can obtain a FHB with an extremely high optical potential and its optimal detuning, which can be used to form a desired atomic lens with a higher resolution and a lower photon-scattering rate. In this case, the aberration from the spontaneous-emission (or photon-scattering) effect can be neglected, and other deBroglie wave aberrations of atomic lenses, such as spherical, dipole, and diffraction aberrations, should be considered. Under this case of high relative aperture, the intensity distribution of the FHB should be calculated by use of the Rayleith–Sommerfeld diffraction theory, which will be considered in our next study.

In addition, when a molecule with two electronic states moves in an inhomogeneous light field, it will also experience an optical dipole force, which is described by an optical trapping potential[27]:

$$U(r) = \frac{\hbar(\omega - \omega_0)}{2}\ln\left[1 + \frac{\Omega^2(r)/2}{(\omega - \omega_0)^2 + (\Gamma/2)^2}\right], \quad (10)$$

where $\omega$ and $\omega_0$ are the laser and molecular resonant frequencies, $\delta = \omega - \omega_0$ is the detuning of the laser field, $\Gamma$ is the natural linewidth of the molecular transition, $\Omega = d_{mol}E/\hbar$ is the Rabi frequency, and $d_{mol}$ is the transition dipole moment of the molecule. When the light field is blue detuned ($\delta > 0$), the optical potential is repulsive, and the cold molecules will be repelled to the minimum of the light field. Therefore the blue-detuned FHB can also be used to guide the cold molecules, even to focus the guided cold molecular beam as a molecular lens.

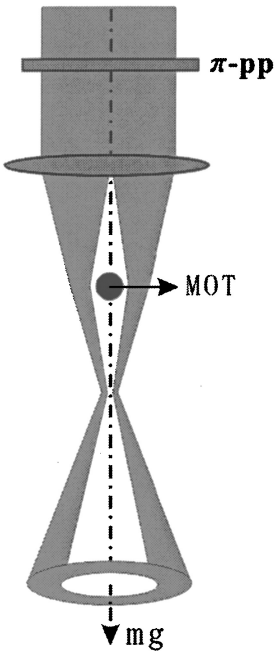


Fig. 10. Principle experimental setup for the study of adiabatic heating and cooling effects of atoms due to the adiabatic compression and expansion of guided atomic beam in the blue-detuned FHB. $\pi$-pp and MOT stand for the $\pi$-phase plate and the magneto-optical trap, respectively.

### C. Study of Adiabatic Heating and Cooling Effects of Cold Atoms (or Molecules)

By using the converging and diverging properties of the FHB before and after the focal point of the lens, the dynamic processes of adiabatic compression (i.e., the adiabatic heating effect) and adiabatic expansion (i.e., the adiabatic cooling effect) of the guided atomic (molecular) beam in the FHB, and the principle experimental scheme is shown in Fig. 10. In experiment, a MOT (or a cold molecular sample) is first prepared at $z = f/2$ after the lens, and then cold atoms (molecules) are released from the MOT (or cold molecular sample); they will fall down under the action of the gravity field and guided in the FHB. Before the focal point of the lens, the DSS of the FHB becomes smaller and smaller, and its intensity gradient becomes larger and larger; the falling process of the guided cold atoms (molecules) is an adiabatically compressed one that results in an adiabatic heating effect of cold atomic (molecular) beams in a convergant hollow beam. However, when the atomic (molecular) beam passes through the focal point of the lens (i.e., after the focal point of the lens), the result is just the opposite; the falling process of the guided cold atoms (molecules) is an adiabatically expanded one that results in an adiabatic cooling effect of cold atomic (molecular) beams in a divergent hollow beam. Therefore our FHB can be used to study dynamic processes of the adiabatic compression and the adiabatic expansion of guided atomic (molecular) beam, which is similar to the case of the guided atomic beam in a focused Gaussian beam.[28]

## 6. CONCLUSIONS

In this paper, we proposed a new scheme to generate a FHB by use of an azimuthally distributed $2\pi$-phase plate, calculated the intensity distributions of the FHB in free propagation space, and studied the relationships between the DSS of the FHB and the waist $w$ of the incident Gaussian beam (or the focal length $f$ of the thin lens). Our study find that before the focal point of the lens, with an increase of the propagation distance $z$, the DSS of the FHB is first increased and then decreased, and there is a maximum DSS at the position of $z = -f/2$. At the focal point, if the lens with a shorter focal length $f$ and the incident laser beam with a larger waist $w_0$ are chosen, the FHB with an extremely small DSS can be obtained. After the focal point, the FHB is propagated with a constant divergent angle, and the DSS of the FHB becomes larger and larger, and its intensity becomes weaker and weaker. We also calculated the optical potential of the blue-detuned FHB for two-level $^{85}$Rb atoms and found that in the focal plane of $z = 0$, the greater the relative aperture $\beta$ of the optical system is, the smaller the DSS of the FHB is, the higher the optical potential is, and the greater the corresponding optimal detuning $\delta$ is, which are beneficial qualities to atomic lenses because they are not only profitable for obtaining an atomic lens with a higher resolution but also helpful for the reduction of the spontaneous photon-scattering effect of atoms in the FHB. Moreover, our FHB can also be used to cool and trap neutral atoms by intensity-gradient induced Sisyphus cooling[24] owing to an extremely high intensity gradient of the FHB itself near the focal point and even to study adiabatic heating and cooling effects of atoms[28] (molecules) because of the adiabatic compression and expansion of guided atomic (molecular) beam in the blue-detuned FHB. Moreover, the blue-detuned FHB can also be used to guide the cold molecules, even to form a molecular lens.

## ACKNOWLEDGMENTS

This work was supported by the National Natural Science Foundation of China under Grants 10434060, 10174050, and 10374029; Shanghai Priority Academic Discipline, and the 211 Foundation of the Educational Ministry of China.

*J. Yin's e-mail address (corresponding author) is jpyin@phy.ecnu.edu.cn.

## REFERENCES

1. H. Ito, K. Sakaki, W. Jhe, and M. Ohtsu, "Atomic funnel with evanescent light," Phys. Rev. A **56**, 712–718 (1997).
2. W. L. Power, L. Allen, M. Babiker, and V. E. Lembessis, "Atomic motion in light beams possessing orbital angular momentum," Phys. Rev. A **52**, 479–488 (1995).
3. H. S. Lee, B. W. Stewart, K. Choi, and H. Fenichel, "Holographic nondiverging hollow beam," Phys. Rev. A **49**, 4922–4927 (1994).
4. N. R. Heckenberg, R. McDuff, C. P. Smith, and A. G. White, "Generation of optical phase singularities by computer-generated holograms," Opt. Lett. **17**, 221–223 (1992).
5. X. Wang and M. G. Littman, "Laser cavity for generation of variable-radius rings of light," Opt. Lett. **18**, 767–768 (1993).
6. J. Yin, H. Noh, K. Lee, K. Kim, Y. Wang, and W. Jhe, "Generation of a dark hollow beam by a small hollow fiber," Opt. Commun. **138**, 287–292 (1997).

7. A. V. Mamaev, M. Saffman, and A. A. Zozulya, "Vortex evolution and bound pair formation in anisotropic nonlinear optical media," Phys. Rev. Lett. **77**, 4544–4547 (1996).
8. V. Tikhonenko and N. N. Akhmediev, "Excitation of vortex solitions in a Gaussian beam configuration," Opt. Commun. **126**, 108–112 (1996).
9. J. Yin, W. Gao, and Y. Zhu, "Generation of dark hollow beams and their applications," Prog. Opt. **44**, 119–204 (2003).
10. V. I. Balykin and V. S. Letokhov, "The possibility of deep laser focusing of an atomic beam into the A-region," Opt. Commun. **64**, 151–156 (1987).
11. G. M. Gallatin and P. L. Gould, "Laser focusing of atomic beams," J. Opt. Soc. Am. B **8**, 502–508 (1991).
12. J. J. McClelland and M. R. Scheinfein, "Laser focusing of atoms: a particle-optics approach," J. Opt. Soc. Am. B **8**, 1974–1984 (1991).
13. Y. Shin, K. Kim, J. Kin, H. Noh, W. Jhe, K. Oh, and U. Paek, "Diffraction-limited dark laser spot produced by a hollow optical fiber," Opt. Lett. **26**, 119–121 (2001).
14. M. W. Beijersbergen, R. P. C. Coerwinkel, M. Kristensen, and J. P. Woerdman, "Helical-wavefront laser beams produced with a spiral phase plate," Opt. Commun. **112**, 321–326 (1994).
15. M. Born and E. Wolf, *Principles of Optics* (Cambridge U. Press, Cambridge, 1980).
16. T. Kazumasa and K. Osamu, "Focus of a diffracted Gaussian beam through a finite aperture lens: experimental and numerical investigations," Appl. Opt. **26**, 390–395 (1987).
17. J. Yin and Y. Zhu, "$LP_{01}$-mode output beam from a micro-sized hollow optical fiber: a simple theoretical model and its applications in atom optics," J. Appl. Phys. **85**, 2473–2481 (1999).
18. H. Ito, K. Sakaki, T. Nakata, W. Jhe, and M. Ohtsu, "Optical potential for atom guidance in a cylindrical-core hollow fiber," Opt. Commun. **115**, 57–63 (1995).
19. J. Yin, Y. Zhu, W. Wang, Y. Wang, and W. Jhe, "Optical potential for atom guidance in a dark hollow laser beam," J. Opt. Soc. Am. B **15**, 25–33 (1998).
20. J. Yin, Y. Zhu, and Y. Wang, "Evanescent light-wave atomic funnel: a tandem hollow-fiber, hollow-beam approach," Phys. Rev. A **57**, 1957–1965 (1998).
21. J. Yin, Y. Zhu, Y. Wang, and W. Jhe, "Atom guiding and cooling in a dark hollow laser beam," Phys. Rev. A **58**, 509–513 (1998).
22. O. Morsch and D. R. Meacher, "Proposal for an optical funnel trap," Opt. Commun. **148**, 49–52 (1998).
23. J. Yin and Y. Zhu, "Dark-hollow-beam gravito-optical atom trap above an apex of a hollow optical fibre," Opt. Commun. **152**, 421–428 (1998).
24. J. Yin, W. Gao, Y. Wang, and Y. Wang, "Improved intensity-gradient cooling of alkali atoms in pyramidal-hollow-beam gravito-optical trap," Phys. Lett. A **288**, 9–15 (2001).
25. Z. T. Lu, K. L. Corwin, M. J. Renn, M. H. Anderson, E. A. Cornell, and C. E. Wieman, "Low-Velocity intense source of atoms from a magneto-optical trap," Phys. Rev. Lett. **77**, 3331–3334 (1996).
26. T. Takekoshi, J. R. Yeh, and R. J. Knize, "Quasi-electrostatic trap for neutral atoms," Opt. Commun. **114**, 421–424 (1999).
27. N. Calander and M. Willander, "Optical trapping of single fluorescent molecules at the detection spots of nanoprobes," Phys. Rev. Lett. **89**, 143603-1-4 (2002).
28. L. Pruvost, D. Marescaux, O. Houde, and H. T. Duong, "Guiding and cooling of cold atoms in a dipole guide," Opt. Commun. **166**, 199–204 (1999).